Preclinical Antilymphoma Activity of a Humanized Anti-CD40 Monoclonal Antibody, SGN-40

Che-Leung Law,[1] Kristine A. Gordon,[1] John Collier,[1] Kerry Klussman,[1] Julie A. McEarchern,[1] Charles G. Cerveny,[1] Bruce J. Mixan,[1] Wyne P. Lee,[2] Zhonghau Lin,[2] Patricia Valdez,[2] Alan F. Wahl,[1] and Iqbal S. Grewal[1,2]

[1]Seattle Genetics, Inc., Bothell, Washington and [2]Department of Immunology, Genentech, Inc., South San Francisco, California

Abstract

SGN-40 is a humanized IgG1 antihuman CD40 that is currently in a phase I clinical trial for the treatment of multiple myeloma. As surface CD40 expression on B-lineage cells is maintained from pro-B cells to plasma cells, SGN-40 may be applicable to treatment of other B-cell neoplasias, including non-Hodgkin's lymphoma. In this study, we examined potential *in vitro* and *in vivo* anti–B-lineage lymphoma activity of SGN-40. Recombinant SGN-40 was expressed and purified from Chinese hamster ovary cells and characterized based on binding affinity, specificity, and normal B-cell stimulation. The ability of SGN-40 to target neoplastic B cells was examined *in vitro* by proliferation inhibition, cytotoxicity, and antibody-dependent cell cytotoxicity assays and *in vivo* by human lymphoma xenograft models. Recombinant SGN-40 showed high affinity, K_d of ~1 nmol/L, and specific binding to CD40. Whereas SGN-40 was a weak agonist in stimulating normal B-cell proliferation in the absence of IL-4 and CD40L, it delivered potent proliferation inhibitory and apoptotic signals to, and mediated antibody-dependent cytotoxicity against, a panel of high-grade B-lymphoma lines. These *in vitro* antilymphoma effects were extended to disseminated and s.c. xenograft CD40 tumor models. In these xenograft models, the antitumor activity of SGN-40 was comparable with that of rituximab. The preclinical *in vitro* and *in vivo* antilymphoma activity of SGN-40 observed in this study provides a rationale for the clinical testing of SGN-40 in the treatment of $CD40^+$ B-lineage lymphomas. (Cancer Res 2005; 65(18): 8331-8)

Introduction

The majority of leukemias and lymphomas originate from malignant transformation of B-lineage cells. As such, they retain most of the phenotypic characteristics of their normal counterparts, including surface expression of B-lineage–restricted leukocyte differentiation antigens. A subset of these antigens, e.g., CD19, CD20, and CD22 are not known to be expressed by normal nonlymphoid cells, making them attractive targets for antibody-based therapeutics for B-cell malignancies.

The best known example is CD20, targeted by the monoclonal antibody (mAb) rituximab. Rituximab has shown safety and efficacy in B-lineage non-Hodgkin's lymphoma as first-line therapy and in relapsed disease and as a single agent or in combination with conventional chemotherapeutics (1). Other Food and Drug Administration–approved, mAb-based therapeutics for B-lineage neoplasias include the humanized anti-CD52 Campath-1H (alemtuzumab; ref. 2) and isotope-labeled anti-CD20 Bexxar ($[^{131}I]$tositumomab; ref. 3) and Zevalin ($[^{90}Y]$ibritumomab tiuxetan; ref. 4). Whereas these new agents have established efficacies in some B-cell malignancies, there is still a significant unmet medical need from patients that do not respond to them. Antibodies against other B-cell–associated surface receptors that can efficiently deplete neoplastic B cells with favorable safety profiles will provide alternative options for lymphoma and leukemia patients resistant to currently approved regimens. One such target on B cells is the tumor necrosis factor (TNF) receptor family member CD40 (5–8).

Within hematopoietic tissues, CD40 is expressed on B-lineage cells from the pro-B to plasma cell stages, monocytes, macrophages, platelets, follicular dendritic cells, dendritic cells, eosinophils, and activated $CD8^+$ T cells. In nonhematopoietic tissues, CD40 is expressed on epithelial cells in the thymus and kidney, keratinocytes, fibroblasts of synovial membrane and dermal origins, and is up-regulated on activated endothelium. In lymphoid malignancies, CD40 is expressed by B-cell precursor acute lymphoblastic leukemia (9), non-Hodgkin's lymphoma (9), Hodgkin's disease (10), and multiple myeloma (11). CD40 is also expressed by carcinomas of the bladder, kidney, ovary, cervix, breast, lung, and nasopharynx as well as malignant melanoma (7, 12, 13). The ligand for CD40 (CD40L) is a member of the TNF superfamily also known as CD154 (5, 8, 14). CD40L is a trimer transiently expressed on activated $CD4^+$, $CD8^+$, and γδ T cells. It is also detected at variable levels on monocytes, activated B cells, epithelial and vascular endothelial cells, smooth muscle cells, dendritic cells, and activated platelets.

CD40/CD40L interaction plays an essential function in contact-dependent interaction between antigen-presenting cells and T cells (14, 15). Mutations in the CD40L locus that abolish functional CD40/CD40L interaction result in the primary deficiency hyper-IgM syndrome (16–19). In contrast, the role of CD40/CD40L interaction in cancer remains to be fully understood. CD40 signaling can be antiapoptotic or proapoptotic on malignant B cells (20). CD40L treatment of some low-grade B-lymphoma cells, e.g., chronic lymphocytic leukemia B cells, promotes cell survival and induction of the costimulatory molecules CD80/CD86 (20, 21). On the other hand, high-grade lymphoma B cells respond to CD40 signaling to undergo growth arrest and apoptosis (22), which may be consequence of Bax (23) and Fas (24) up-regulation.

In this study, we characterized the binding and functional activities of the humanized anti-CD40 mAb SGN-40. SGN-40 shows both *in vitro* and *in vivo* antitumor activities against human B-lymphoma cell lines. We have identified that apoptosis induction due to caspase-3 activation and antibody-dependent cell cytotoxicity

Requests for reprints: Che-Leung Law, Seattle Genetics, Inc., 21823 30th Drive Southeast, Bothell, WA 98021. Phone: 425-527-4612; Fax: 425-527-4609; E-mail: claw@seagen.com.

doi:10.1158/0008-5472.CAN-05-0095

(ADCC) are key mechanisms underlying the antitumor activity of SGN-40. Our findings suggest that SGN-40 may be therapeutically active in clinical settings against CD40-expressing B-lineage lymphomas.

Materials and Methods

Cells and reagents. The B cell lines HT, RL, Toledo, CA46, MC116, Ramos, Daudi, HS-Sultan, Raji, and IM-9 were obtained from the American Type Culture Collection (Manassas, VA). The U-698-M, MHH-PREB-1, and SU-DHL-4 B cell lines were obtained from DSMZ (Braunschweig, Germany).

Resting B cells were enriched from normal peripheral blood mononuclear cells (PBMC) using the Dynal B Cell Negative Isolation kit (Brown Deer, WI), which deplete cells expressing CD2, CD14, CD16, CD36, CD43, and CD235a. Enriched B cells were usually >80% $CD19^+$.

We previously reported SGN-14 (25), which is a chimeric antibody consisting of the V_H and V_L domains of the murine antihuman CD40 mAb S2C6 (26, 27) and human IgG1(κ) constant regions. Subsequent humanization of SGN-14 yielded SGN-40, which contains the complementarity determining regions of murine S2C6 in the human IgG1(κ) framework sequences. SGN-40 is expressed and purified from Chinese hamster ovary cells.

Antibodies against CD19, CD20, CD40, and activated caspase-3 were purchased from BD Biosciences (San Jose, CA). Recombinant human CD40L containing the 149-amino-acid CD40-binding TNF-like domain was purchased from Research Diagnostics (Flanders, NJ).

Affinity of SGN-40 to cell surface CD40. SGN-40 and murine S2C6 were labeled with europium N1-isothiocyanate (Perkin-Elmer Biosciences, Wellesley, MA) overnight at 4°C in 50 mmol/L Na_2CO_3 (pH 9.0). Conjugates were purified into TBS [50 mmol/L Tris-HCl (pH 8.0), 150 mmol/L NaCl] by size exclusion chromatography and then dialyzed overnight in TBS at 4°C. Conjugate concentration was determined by UV absorbance. Europium content was quantified by release into DELFIA enhancement solution (Perkin-Elmer Biosciences) and using time-resolved fluorescence (400-microsecond delay between excitation and emission) on a Fusion HTS microplate reader (Perkin-Elmer Biosciences) at excitation and emission wavelengths of 335 and 620 nm, respectively. Europium loading was usually three to seven molecules per mAb molecule.

To determine K_d, Ramos cells [100 μL/well at 5×10^6/mL in TBS + 0.5% fetal bovine serum (FBS), 10 μmol/L EDTA] were incubated with varying concentrations of labeled mAbs for 1 hour at 4°C with rocking. After three washes in TBS, cells were resuspended in 200 μL of enhancement solution, transferred to DELFIA yellow-sided plates, and incubated on an orbital shaker for 5 minutes at room temperature. Time-resolved fluorescence was measured by a Fusion HTS microplate reader as described above. A minimum of three independent experiments each with quadruplicate determinations was conducted. Saturation binding curves were generated using nonlinear regression and a one-site binding model provided in GraphPad Prism software (GraphPad Software, San Diego, CA) to derive K_d values.

Proliferation assay. B cells were seeded in 96-well flat-bottom plates at 100,000 cells/well in 200 μL RPMI 1640 supplemented with 10% FBS containing varying concentrations of SGN-40 or a control nonbinding chimeric IgG (cIgG). For cross-linking, SGN-40 or cIgG was complexed with $F(ab')_2$ fragments of a goat antihuman IgG Fcγ fragment-specific antibody (Jackson ImmunoResearch, West Grove, PA) in medium for 30 minutes at room temperature before adding to cells. Recombinant human interleukin (IL)-4 (R&D Systems, Minneapolis, MN) and recombinant CD40L were supplemented in some cultures at final concentrations of 10 ng/mL and 1 μg/mL, respectively. Cells were stimulated for a total of 72 hours. DNA synthesis was assessed by pulsing with [^{3}H]thymidine, 0.5 μCi per well, during the last 16 hours of incubation. B cell lines were seeded in 96-well flat-bottomed plates at 25,000 cells/well in 200 μL RPMI 1640 supplemented with either 2% or 10% FBS containing graded concentrations of SGN-40 or cIgG. Cross-linking of SGN-40 and cIgG was done as described above. Incubation was carried out for a total of 72 hours. DNA synthesis was assayed by [^{3}H]thymidine incorporation during the last 16 hours of incubation.

Flow cytometry and apoptosis analysis. For indirect staining, 2×10^5 cells were incubated with 50 μL of staining medium (RPMI 1640, 5-10% FBS, 0.02% NaN_3) containing 10 μg/mL of primary antibodies. After incubation on ice for 20 to 30 minutes, cells were washed with staining medium and counterstained for 20 to 30 minutes on ice with FITC-conjugated goat antimouse IgG or FITC-conjugated goat antihuman IgG (Jackson ImmunoResearch), washed thrice, and fixed in PBS containing 1% paraformaldehyde before analysis on a FACScan (BD Immunocytometry, San Jose, CA). For direct staining, 2×10^5 cells were incubated in staining medium (RPMI 1640, 5-10% FBS, 0.02% NaN_3) containing 10 μg/mL of mAb on ice, washed, and fixed as described above before analysis on a FACScan (BD Biosciences). For apoptosis analysis, the Annexin V-FITC Apoptosis Detection kit (Oncogene Research Products, La Jolla, CA) was used according to the instructions of the manufacturer.

Caspase-3 activation. After treatment of Ramos cells with cross-linked SGN-40 or camptothecin, cells were fixed in paraformaldehyde and permeabilized with saponin using the Perm/Fix buffer (BD Biosciences). Activation of caspase-3 was detected using flow cytometry with an antibody recognizing only the cleaved, enzymatically active fragment of caspase-3 (BD Biosciences) according to the instructions of the manufacturer.

Antibody-dependent cell cytotoxicity assay. Target cells were labeled with 100 μCi $Na^{51}CrO_4$ for 1 hour at 37°C and adjusted to a concentration of 7.2×10^4/mL in RPMI containing 1% heat inactivated FBS. Seventy microliters of target cells were preincubated with graded concentrations of antibody for 30 minutes before addition of effector cells. To prepare effector cells, cryopreserved PBMCs from normal donors were cultured overnight in AIMV medium containing 5% heat inactivated human serum. Nonadherent cells were collected and adjusted to reflect $CD16^+$ cells as determined by flow cytometry. Viable $CD16^+$ cells were added to targets at an effector-to-target cell ratio of ~15:1. After 4 hours incubation at 37°C, supernatants were collected and analyzed for radioactivity. Percentage cytotoxicity was calculated as: [test cpm − spontaneous cpm] / [total cpm − spontaneous cpm] × 100. Spontaneous release was determined from the supernatant of target cells incubated in assay medium alone. Total release was determined from labeled cells lysed with 2% Triton X-100. Data are expressed as the mean of triplicate wells.

***In vivo* tumor xenograft models.** In the disseminated disease models, 1×10^6 Ramos or IM-9 cells were inoculated into C.B-17/lcr-SCID mice by i.v. injections. Three days after tumor cell inoculation, mice (10 per group) were treated with i.p. injections of antibodies. Inoculation with Ramos or IM-9 cells resulted in 100% mortality of control mice by study days 30 to 40 or study days 40 to 60, respectively. Median survival and Kaplan-Meier survival curve comparison using a log-rank test was conducted with the GraphPad Prism software. Mice that survived until the end of the study (90 and 66 days post tumor implant for Ramos and IM-9, respectively) were censored. In the second model, 5×10^6 Ramos cells were implanted s.c. into severe combined immunodeficient (SCID) or SCID-beige mice and allowed to establish as tumors for 13 days before the start of antibody treatment by i.p. injections. Tumor dimensions were determined by caliper measurements and tumor size was calculated using the formula (length × width^2) / 2. Experiments were terminated 2 or 3 weeks after the start of the treatment for the SCID model or SCID-beige model, respectively. Student's t test was used to compare tumor sizes between the treatment and control groups. All animal experiments were conducted under Institutional Animal Care and Use Committee guidelines and approval.

Results

Characterization of SGN-40. SGN-40 and its parent murine S2C6 gave overlapping binding curves when tested on the $CD40^+$ Burkitt's lymphoma cell line Ramos; both antibodies saturated Ramos cells around 0.4 μg/mL (Fig. 1*A*). In sequential addition experiments, SGN-40 and S2C6 completely cross-blocked each other's binding to target cells, indicating that humanization of S2C6 did not significantly alter its antigen binding paratope (data not shown).

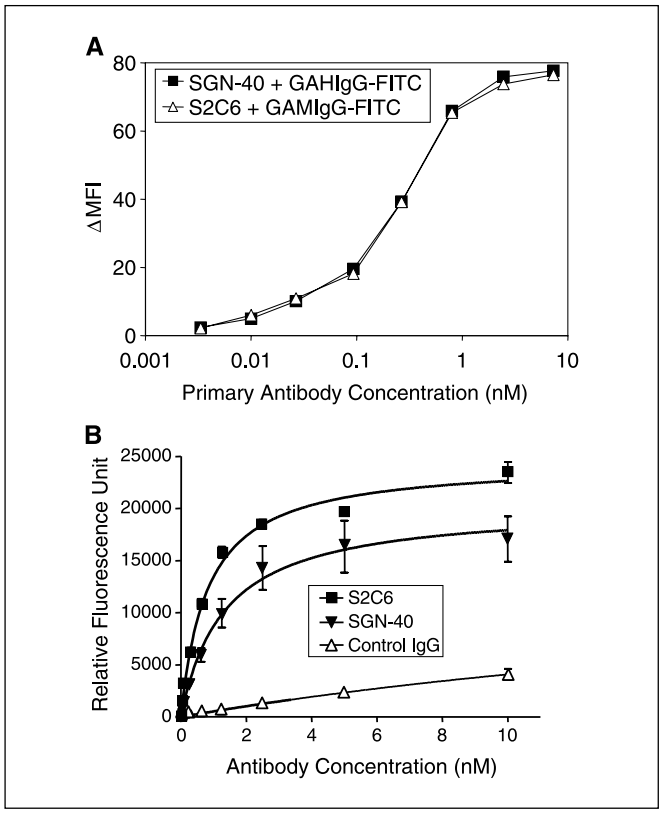

Figure 1. Binding characteristics of SGN-40 and S2C6. *A,* binding of SGN-40 and S2C6 to Ramos B-lymphoma cells was determined by indirect immunofluorescence staining and flow cytometry. Background-subtracted mean fluorescence intensity (*ΔMFI*) was plotted against the mAb concentrations. *B,* an equilibrium saturation binding assay as described in Materials and Methods was used to determine the K_d values for SGN-40 and S2C6 to CD40 expressed by Ramos cells. Representative binding curves generated from the means of three independent experiments are shown. In each experiment, quadruplicate determinations were done for each concentration of labeled antibody used. *Points,* mean; *bars,* SE.

A cell-based assay was used to determine the affinity of SGN-40 for CD40, as shown by the saturation binding curves obtained for both SGN-40 and S2C6 (Fig. 1*B*). By subtracting nonspecific binding of the IgG control in combination with nonlinear regression analysis, K_d values for SGN-40 and S2C6 were found to be within 2-fold of each other, at 1.00 ± 0.20 and 0.65 ± 0.08 nmol/L, respectively. These data confirmed that humanization of S2C6 had minimal impact on specificity and affinity toward CD40.

Effects of SGN-40 on normal B cells. Anti-CD40 mAbs can be classified as agonists, antagonists, or partial agonists based on their B-cell stimulatory activities (28, 29). SGN-40 up to 10 μg/mL did not stimulate proliferation of resting B cells and IL-4 did not costimulate with SGN-40 (Fig. 2*A, top*). Cross-linking SGN-40 with a secondary antibody to simulate *in vivo* antibody cross-linking by Fcγ receptor (FcγR)-expressing cells only marginally augmented its stimulatory activity at concentrations ≥0.1 μg/mL (Fig. 2*A, bottom*). As a positive control for the proliferation capacity of the normal B cells, cross-linked SGN-40 combined with IL-4 stimulated significant DNA synthesis (Fig. 2*A, bottom*).

We previously reported that a chimeric form of S2C6 (SGN-14) stimulated primary B-cell proliferation when both CD40L and IL-4 were present (25). SGN-40 has retained this activity to costimulate normal B cell with functional recombinant CD40L and IL-4 (Fig. 2*B*). It is noteworthy that SGN-40 with CD40L showed minimal costimulation, as did SGN-40 plus IL-4, and both combinations were weaker than CD40L plus IL-4. More importantly, cross-linked SGN-40 also showed minimal costimulation with CD40L. Agonistic activity of CD40L was confirmed by its activity to costimulate when both SGN-40 and IL-4 were present. Experiments in Fig. 2 also show that B-cell proliferation was induced only by a combination of SGN-40, IL-4, and CD40L or cross-linked SGN-40 with IL-4. As cells used in this study were not 100% B cells, part of the proliferation response could be due to contaminating non-B cells. Thus, SGN-40 alone is a

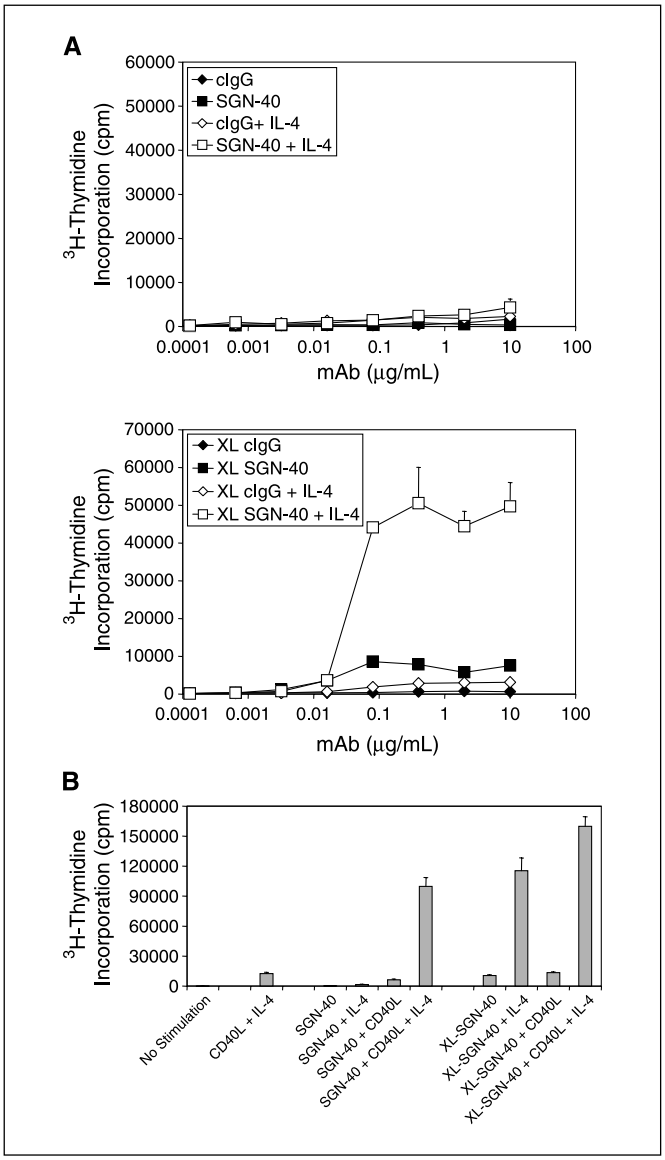

Figure 2. Agonistic activity of SGN-40 on normal B cells. *A,* B cells enriched from PBMCs were treated with increasing concentrations of SGN-40 or a nonbinding control IgG (cIgG) with (*bottom*) or without (*top*) secondary cross-linking (*XL*) by the F(ab')$_2$ fragments of a goat antibody specific for the Fcγ fragment of human IgG. IL-4 (10 ng/mL) was also tested. Cells were stimulated for a total of 72 hours and proliferation was detected by pulsing with [^{3}H]thymidine during the last 16 hours of incubation. *Bars,* SDs from triplicate determinations. *B,* B cells enriched from PBMCs were treated with SGN-40 or a control nonbinding IgG (cIgG) with or with secondary cross-linking. The effects of IL-4 (10 ng/mL), recombinant CD40L (1 μg/mL), or IL-4 plus recombinant CD40L in combination with SGN-40 were also tested. Cells were stimulated and proliferation as in (*A*). *Bars,* SDs from triplicate determinations.

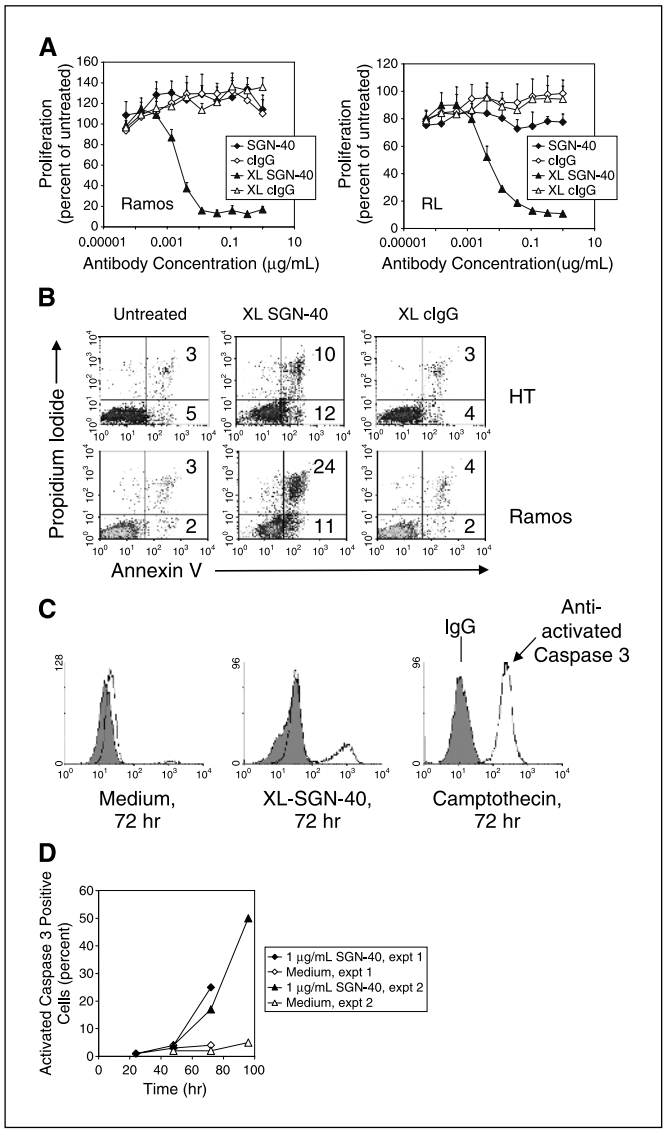

Figure 3. Growth inhibitory and apoptotic effects of SGN-40 on non-Hodgkin's lymphoma B cell lines. *A,* Burkitt's lymphoma B cell line (Ramos, *left*) and non-Hodgkin's lymphoma B cell line (RL, *right*) were incubated with graded doses of SGN-40 or a nonbinding control IgG (cIgG) with or without cross-linking by the F(ab')$_2$ fragments of a goat antibody specific for the Fcγ fragment of human IgG in medium containing 2% FBS. Proliferation was determined by [^{3}H]thymidine incorporation during the last 16 hours of culture. Proliferation as percentages of the untreated control was plotted against mAb concentrations. The average [^{3}H]thymidine incorporation in untreated Ramos and RL cells was 174,000 and 184,000 cpm, respectively. The concentration of mAb that inhibited thymidine incorporation by 50% is defined as the IC_{50}. *Bars,* SDs from quadruplicate determinations. *B,* HT and Ramos cells were incubated in medium containing 2% FBS with 1 μg/mL of SGN-40 or 1 μg/mL of a nonbinding control IgG (cIgG) cross-linked as described in (*A*). Cells were incubated for a total of 72 hours. Flow cytometry was used to analyze for Annexin V binding and PI permeability. The percentages of apoptotic (Annexin V$^+$/PI$^-$) and dead (Annexin V$^+$/PI$^+$) are indicated by the numbers in the corresponding quadrants. *C,* Ramos cells treated in medium containing 2% FBS with 12 μmol/L of camptothecin or 1 μg/mL of cross-linked SGN-40 as in (*A*). After 72 hours of incubation, cells were examined for the presence of activated caspase-3 by flow cytometry. *D,* kinetics of SGN-40–induced caspase-3 activation was examined in Ramos cells as described in (*C*).

weak agonist for normal resting B cells. In situations where IL-4 is not available, SGN-40 will not stimulate B-cell expansion although it may be cross-linked by FcγR-expressing cells and in the presence of CD40L.

***In vitro* effects of SGN-40 on lymphoma B-cell proliferation.** Ligation of CD40 on high-grade lymphoma B cells generally results in proliferation inhibition (20, 22, 23). Soluble SGN-40 did not affect proliferation of B-lymphoma cell lines. When SGN-40 at concentrations ranging from <0.1 ng/mL to 1 μg/mL was cross-linked by a secondary antibody, it delivered a dose-dependent proliferation inhibitory effect to B-lymphoma lines. Representative dose-response curves for the Burkitt's lymphoma cell line (Ramos) and the non-Hodgkin's lymphoma cell line (RL) are shown (Fig. 3*A*). In both cell lines, cross-linked SGN-40 reduced proliferation to <25% of the control untreated cells.

Thirteen B-lymphoma lines were tested for their response to cross-linked SGN-40 (Table 1). When tested in medium containing 2% FBS, the maximum proliferation inhibitory activity of cross-linked SGN-40 ranged from 25% to 90%, with the exception of Raji, whose proliferation was unaffected. Usually <0.1 μg/mL of cross-linked SGN-40 was needed to achieve maximum inhibition. In cell lines where an IC_{50} was reached, its value was in the range of 0.01 to 0.1 μg/mL. Efficacy was reduced when cross-linked SGN-40 was added to cells maintained in medium containing 10% FBS. Nine of the 13 cell lines showed 30% to 80% proliferation inhibition, and the remaining four were not affected.

SGN-40–induced apoptosis and caspase-3 activation in B-lymphoma cell lines. Proliferation inhibition mediated by SGN-40 in HT, Ramos, RL, and MHH-PREB-1 cells was accompanied

Table 1. Proliferation inhibitory activity of SGN-40 on B-lymphoma cell lines

Lymphoma cell lines	Maximum percentage of proliferation inhibition induced by SGN-40*	
	2% FBS	10% FBS
Diffuse large cell		
HT	80	0
Toledo	40	0
Lymphoblastic		
RL	80	40
U-698-M	ND	40
EBV-negative Burkitt's lymphoma		
CA46	50	0
MC116	70	40
MHH-PREB-1	90	60
Ramos	90	50
SU-DHL-4	90	80
EBV-positive Burkitt's lymphoma		
Daudi	70	40
HS-Sultan	50	30
Raji	0	30
EBV-transformed LCL		
IM-9	25	0

Abbreviations: ND, not determined; LCL, lymphoblastoid cell line.
*Non-Hodgkin's lymphoma B cell lines were examined for their responses to cross-linked SGN-40 (0.1 ng/mL-1 μg/mL) by [^{3}H]thymidine incorporation assay as described in Fig. 3*A*. Cells were maintained in either 2% or 10% FBS containing medium during assay. The maximum percentage of proliferation inhibition induced by cross-linked SGN-40 is tabulated.

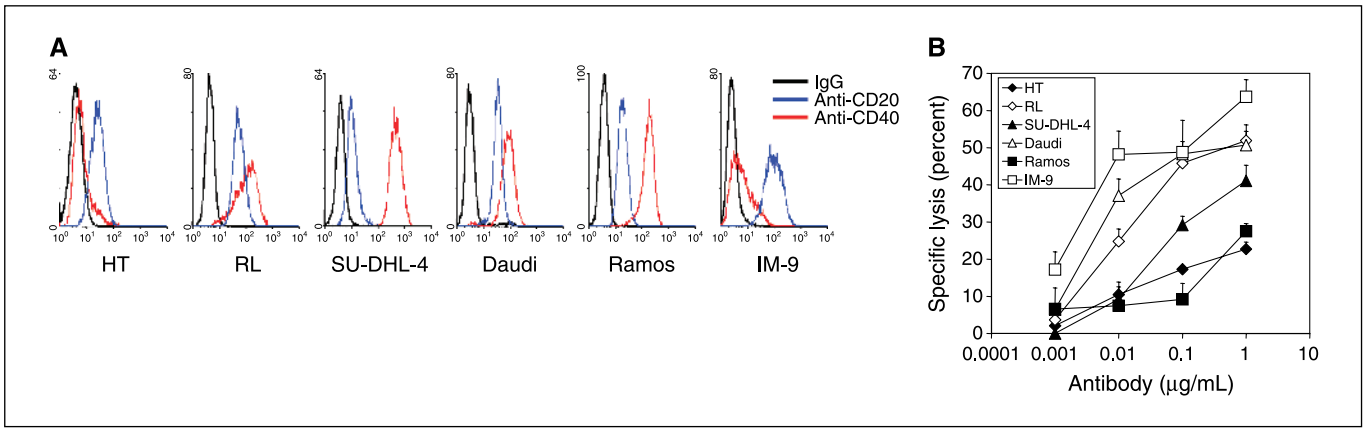

Figure 4. SGN-40–mediated ADCC. *A,* surface expression of CD20 and CD40 on target B cell lines was determined by flow cytometry. *B,* specific lysis of target cells in an ADCC assay at graded doses of SGN-40 using normal PBMCs as effector cells was determined. Specific lysis of HT, RL, SU-DHL-4, Daudi, Ramos, and IM-9 by 1 μg/mL of the control mAb rituximab was 0.2%, 49%, 23.5%, 58.4%, 51.7%, and 37.1%, respectively.

by apoptosis. Using Annexin V binding and propidium iodide (PI) permeability as readouts for apoptotic and dead cells, both HT and Ramos cell undergo apoptosis following SGN-40 treatment (Fig. 3*B*). For RL and MHH-PREB-1 cells, the percentages of total Annexin V^+ cells were 14 and 24, compared with the control cIgG-treated cells of 6 and 9, respectively.

Similar to camptothecin, treatment of Ramos cells with cross-linked SGN-40 induced caspase-3 activation (Fig. 3*C, middle*). Kinetic analysis revealed that Ramos cells needed to be exposed to cross-linked SGN-40 for >48 hours before caspase-3 activation could be observed (Fig. 3*D*). At 96 hours, ~50% of the SGN-40–treated cells became positive for activated caspase-3, compared with <5% of cells kept in medium. Caspase-3 activation was also detected in RL and HT cells. After 96 hours of SGN-40 treatment, 7% and 28% RL and HT cells expressed activated caspase-3, respectively, compared with 2% and 12%, respectively, in control cells.

SGN-40–mediated antibody-dependent cell cytotoxicity on B-lymphoma cell lines. Because SGN-40 mediates ADCC on $CD40^+$ multiple myeloma cells (30), we examined if B-lymphoma cell lines were also susceptible to SGN-40–mediated ADCC. Relative levels of CD40 expression on HT, RL, SU-DHL-4, Daudi, Ramos, and IM-9 lines is shown in Fig. 4*A*. Whereas RL, SU-DHL-4, Daudi, and Ramos expressed CD20, IM-9 was weakly $CD20^+$, and HT was essentially $CD20^-$ (Fig. 4*A*). Using PBMC as effector cells, SGN-40–mediated ADCC in a dose-dependent fashion. Significant cytotoxicity was observed when SGN-40 was ≥0.01 μg/mL. At the maximum dose of 1 μg/mL of SGN-40, specific lysis of target cells ranged from 20% to >50% (Fig. 4*B*). SGN-40 did not mediate any ADCC on $CD40^-$ target cells, confirming the specificity of SGN-40 for CD40 (data not shown). The positive control rituximab also effectively lysed the $CD20^+$ targets RL, SU-DHL-4, Daudi, Ramos, and IM-9 but not the $CD20^-$ target HT (Fig. 4*B*).

***In vivo* antitumor activities of SGN-40.** In a disseminated Ramos model, control group animals did not survive beyond study day 34 (Fig. 5*A*). Using a less frequent dosing schedule and fewer total doses compared with experiments shown in Fig. 5*C* and *D*, a clear dose-dependent effect of SGN-40 on promoting survival was observed. Significant survival advantage was observed even at the lowest dose of 0.04 mg/kg. Median survival improved from 28 days in the control group to 55.5 days in the group treated with 0.04 mg/kg/dose of SGN-40, and median survival for the groups treated with higher doses of SGN-40 was >90 days. In a disseminated IM-9 model, SGN-40 was compared with rituximab. In the control group, 100% mortality was observed by day 49 postinoculation (Fig. 5*B*). Similar to the Ramos model, SGN-40 significantly improved survival. Although IM-9 express relatively low levels of CD20 (Fig. 4*A*), rituximab also improved survival. The median survival for the control group, SGN-40–treated group, and rituximab-treated group, was 28, 64.5, and 43.5 days, respectively.

The efficacy of SGN-40 against Ramos was further examined in a s.c. implant model. Antibody administrations started when tumors reached ~100 mm^3, usually on day 13 postimplantation. In the control group, tumor sizes increased rapidly to >1,500 mm^3 within 4 weeks (Fig. 5*C*). Mice treated with either SGN-40 or the positive control rituximab had minimal tumor growth, demonstrating once again similar antitumor activity between SGN-40 and rituximab. The role of SGN-40–mediated ADCC in the suppression of *in vivo* Ramos tumor growth was evaluated by using the SCID-beige strain of mice that has impaired natural killer (NK)-mediated ADCC activity (31, 32). Despite defective NK activity of the SCID-beige mice, SGN-40 suppressed Ramos tumor growth in these hosts with similar potency seen in C.B-17/Icr-SCID hosts (Fig. 5*C* and *D*). On the other hand, the efficacy of rituximab seemed to be reduced. Compared to the SGN-40–treated mice, tumors in the rituximab-treated mice were significantly larger on days 25, 31, and 38 (Fig. 5*D*).

Discussion

We have previously reported a chimeric anti-CD40 mAb, SGN-14, derived from the murine mAb S2C6 (25). SGN-14 was subsequently humanized to yield SGN-40. SGN-40 mediates ADCC against multiple myeloma cells (30) as well as down-modulates expression of the IL-6 receptor on multiple myeloma cells leading to reduced response to IL-6–induced survival and proliferation (33). Together with the safety profile established in nonhuman primates,[3] a phase I clinical trial on SGN-40 in multiple myeloma was initiated.

In this study, we analyzed the binding and functional properties of SGN-40. The K_d of SGN-40 binding to native CD40 expressed on cell surface was found to be around 1 nmol/L, similar to its parent

[3] S.K. Kelley, et al. Preclinical pharmacokinetics, pharmacodynamics, and safety of a humanized anti-CD40 antibody (SGN-40), submitted.

murine mAb, S2C6. This value compares favorably to the affinity of rituximab and epratuzumab to their target antigens, at 8 nmol/L (rituximab drug package insert) and 0.7 nmol/L (34), respectively. SGN-40 and S2C6 recognize the same epitope as revealed by cross-blocking experiments. Costimulation experiment showed that SGN-40 is a weak agonist for resting B cells (Fig. 2) as reported for SGN-14 (25). We conclude that SGN-40 has retained the characteristics of its parental antibodies SGN-14 and murine S2C6.

CD40 signaling can induce either proliferation or apoptosis among B-lineage cells. Ligation of CD40 on a murine lymphoma cell line inhibits proliferation (35). An antiserum against murine CD40 stimulated normal splenic B cells to proliferate, whereas it inhibited proliferation of B-lymphoma lines, leading to the hypothesis that anti-CD40 may be therapeutically efficacious against B lymphomas (36). In both murine (37) and human B-lineage cells (20, 22), lymphoma lines derived from mature B cells are more sensitive to CD40-induced apoptosis than those derived from immature B cells. Our observation that SGN-40 delivers proliferation inhibitory and apoptosis signals to a panel of B-lymphoma lines originated from high-grade non-Hodgkin's lymphoma (Fig. 3; Table 1) is consistent with these findings.

Cross-linking is required for SGN-40 to exert its cytotoxicity (Fig. 3; Table 1); hence, efficient CD40 signaling depends on receptor oligomerization. This is consistent with the trimeric nature of CD40L. We hypothesize that *in vivo* cross-linking of SGN-40 resulted from interaction of the Fc portion of SGN-40 with FcγR-expressing cells within the hematopoietic and reticulo-endothelial systems, which is required for efficient SGN-40 signaling to lymphoma cells. Such interaction was simulated by the complex formation between SGN-40 and the secondary cross-linking antibody used in this study.

We also identified caspase-3 activation as an intermediary step in SGN-40–mediated lymphoma B-cell apoptosis (Fig. 3). Fas-FasL interaction has been reported to trigger CD40-mediated apoptosis in both epithelial and hematopoietic cells (24, 38–40). Similar to other anti-CD40 mAbs (24), cross-linked SGN-40 up-regulated expression of Fas on B-lymphoma cells (data not shown). However, we did not observe FasL expression on SGN-40–treated B-lymphoma cells, and a neutralizing anti-FasL antibody did not suppress SGN-40–induced apoptosis in these cells (data not shown), suggesting a Fas-independent mechanism(s) for caspase-3 activation. Because CD40-mediated apoptosis has been correlated to Bax induction (23), a mitochondrial pathway for SGN-40–induced caspase-3 activation is possible. Alternatively, up-regulation of p53 by CD40 signaling may also lead to growth arrest and caspase-3 activation in transformed B cells (37, 41).

Stronger proliferation inhibition was delivered by SGN-40 to B-lymphoma cells maintained in medium containing 2% compared with 10% FBS (Table 1). Hence, limiting the overall growth capacity of B-lymphoma cells may enhance the cytotoxicity of SGN-40. In some carcinoma (24, 38–40) and multiple myeloma (33) cell lines, CD40 ligation alone does not induce apoptosis. Interestingly, target cells can be sensitized by a noncytotoxic dose of the protein synthesis inhibitor cycloheximide and become susceptible to

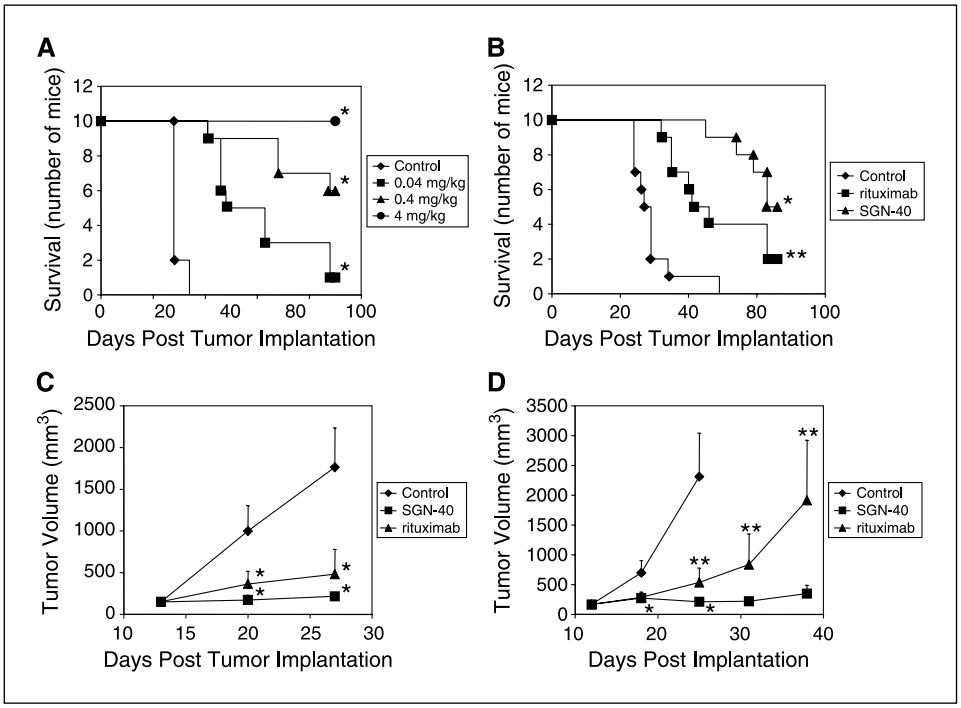

Figure 5. *In vivo* antitumor activity of SGN-40. *A,* SCID mice (n = 10/group) were inoculated (i.v.) with 1×10^6 Ramos cells 3 days before drug treatment. SGN-40 was administered at graded doses of 0.04 (~0.8 μg/mouse), 0.4 (~8 μg/mouse), or 4 mg/kg/dose (~8 μg/mouse) via i.p. injections twice per week for a total of five doses. The nonbinding control mAb (*Control*) was administered at 4 mg/kg/doses using the same schedule. *, $P \leq 0.001$ when compared with the control group. *B* SCID mice (n = 10/group) were inoculated (i.v.) with 1×10^6 IM-9 cells 3 days before drug treatment. SGN-40, rituximab, or a nonbinding control mAb was given by i.p. injections thrice per week (4 mg/kg/dose) for a total of nine doses. P values between the control group and the SGN-40– and rituximab treated groups are ≤0.0001 (*) and 0.0008 (**), respectively. *C,* SCID mice (n =10 per group) were transplanted with 5×10^6 Ramos cells (s.c.) 13 days before starting drug treatment. SGN-40 or rituximab was given by i.p. injections thrice per week (4 mg/kg/dose) for a total of nine doses. *Points,* mean; *bars,* SD. *, $P \leq 0.0001$ when compared with the corresponding time points of the control group. *D,* SCID-beige mice (n =10 per group) were inoculated (s.c.) with 5×10^6 Ramos tumor cells 3 days before drug treatment. SGN-40, rituximab, or a control nonbinding mAb was given by i.p. injections thrice per week (4 mg/kg/dose) for a total of nine doses. *Points,* mean; *bars,* SD. *, $P < 0.001$ when compared with the corresponding time points of the control group. **, $P < 0.002$ when compared with the SGN-40–treated group.

CD40-induced apoptosis (24, 33, 38–40), suggesting that SGN-40 in combination with chemotherapeutics may provide improved therapeutic efficacy relative to SGN-40 alone. A key downstream survival pathway triggered by CD40 is activation of nuclear factor (NF)-κB (42, 43). Agents that dampen NF-κB activity may deliver similar effects as serum deprivation or cycloheximide stress. In view of this, down-modulation of NF-κB by thalidomide and its derivatives (44), the proteasome inhibitor Velcade (45), the IκB kinase inhibitor Trisenox (46), is a potential strategy to enhance SGN-40–mediated apoptosis in lymphoma B cells.

SGN-40 shows potent antitumor activity against xenograft lymphomas (Fig. 5). At the doses and schedules used in these models, the efficacy of SGN-40 is comparable with that of rituximab (Fig. 5*C*; and data not shown). Antihuman CD40 mAbs have been reported to delay tumor progression in xenograft models of human non-Hodgkin's lymphoma (22, 25, 47). Of interest is the results obtained from the human peripheral blood lymphocyte (huPBL)-SCID model. Transfer of normal huPBL from EBV-seropositive donors into SCID mice results in the emergence of human B-cell lymphomas in the hosts. Treatment with the anti-CD40 M3 prevents lymphoma generation, whereas permitting engraftment of functional normal human B cells (48, 49). Existing B-cell depletion modalities involving anti-CD20 and anti-CD52 mAbs indiscriminately eliminate both normal and transformed B cells. It is possible that anti-CD40 mAbs may preferentially deplete lymphoma B cells while sparing normal B cells and, hence, have reduced impact on humoral immune repertoire of patients.

Despite the lack of complement-dependent cytotoxicity in SGN-40 (data not shown), *in vitro* and *in vivo* studies suggest that both apoptotic signaling and antibody effector function via ADCC contribute to antitumor activity of SGN-40. Ramos cells was susceptible to SGN-40–mediated apoptosis, but was a relatively poor target in ADCC assays (<30% specific lysis at saturating SGN-40; Fig. 4*B*). In three different xenograft models, SGN-40 showed significant antitumor activity, supporting the hypothesis that SGN-40–mediated apoptosis may be the principal mechanism of *in vivo* Ramos xenograft ablation. The activity seen in the NK-deficient SCID-beige host further supports this hypothesis. Although other FcγR-expressing cells, e.g., macrophages, may play a role in the antitumor effects of SGN-40 in SCID-beige hosts, our results are consistent with previous reports that reducing host NK activity through antibodies against asialo-GM1 (25) or Fc receptors (47) only had marginal impact the antitumor activities of other anti-CD40 mAbs. On the other hand, whereas IM-9 cells were good targets for SGN-40–mediated ADCC, they were refractive to SGN-40 in proliferation assay. IM-9 xenografts were also susceptible to SGN-40 treatment; thus, it is likely that ADCC is the predominant mechanism for the *in vivo* efficacy of SGN-40 against IM-9 cells. Studies are currently in progress to more precisely delineate the relative contribution of cytotoxic signaling and ADCC in the *in vivo* efficacy of SGN-40 using xenograft models established from cell lines with varying degrees of susceptibilities toward SGN-40–mediated apoptosis and ADCC.

SGN-40 may offer a therapeutic option for patients who have failed treatments based on antibodies against CD20 and CD52. Recent analysis of using FcγR-deficient mice in xenograft models (50) and polymorphism at the human *FCGR3A* gene locus (51, 52) has revealed that FcγRIII-dependent, effector cell–mediated functions are important for rituximab to deplete B cells. Whereas patients homozygous for the allele encoding high affinity FcγRIIIA (V158) show a significantly higher response rate to rituximab, patients homozygous for the allele encoding low-affinity FcγRIIIA (F158) or patients heterozygous at this locus are more resistant to rituximab treatment (51, 52). It is possible that direct cytotoxic signaling by SGN-40 to lymphoma B cells may provide substantial therapeutic activity to patients who have suboptimal FcγRIIIA-mediated immune effector cell functions due to the presence of low-affinity FcγRIIIA. CD40 also has a broader expression pattern than the B cell–restricted CD20 receptor. B-lymphoma aside, CD40 is expressed by a subset of B-cell precursor acute lymphoblastic leukemia, multiple myeloma, Reed-Sternberg cells of Hodgkin's disease, malignant melanoma as well as carcinomas of a variety of tissues. As a result, SGN-40 may be applicable for treatment of both hematopoietic and nonhematopoietic malignancies.

Proliferation assays clearly showed that monomeric SGN-40 did not stimulate normal B cells (Fig. 2). The limited proliferation response recorded in resting B cells treated with cross-linked SGN-40 would imply that SGN-40 probably will not stimulate extensive *in vivo* B-cell expansion even in the presence of FcγR-bearing cells. This is supported by the observation that SGN-40 does not stimulate overt *in vivo* B-cell proliferation in nonhuman primates.[3] Furthermore, neither monomeric nor cross-linked SGN-40 activated monocytes freshly isolated from PBMC (data not shown). Hence, systemic administrations of SGN-40 will most likely have minimal or no activating effect on circulating $CD40^+$ hematopoietic cells. In summary, the safety profile of SGN-40 and its *in vitro* and *in vivo* antilymphoma activity in both preclinical models provide a rationale for clinical testing of SGN-40 on $CD40^+$ non-Hodgkin's lymphoma.

Acknowledgments

Received 1/11/2005; revised 6/30/2005; accepted 7/8/2005.

The costs of publication of this article were defrayed in part by the payment of page charges. This article must therefore be hereby marked *advertisement* in accordance with 18 U.S.C. Section 1734 solely to indicate this fact.

References

1. Rastetter W, Molina A, White CA. Rituximab: expanding role in therapy for lymphomas and autoimmune diseases. Annu Rev Med 2004;55:477–503.
2. Robak T. Monoclonal antibodies in the treatment of chronic lymphoid leukemias. Leuk Lymphoma 2004;45:205–19.
3. Vose JM. Bexxar: novel radioimmunotherapy for the treatment of low-grade and transformed low-grade non-Hodgkin's lymphoma. Oncologist 2004;9:160–72.
4. Chinn P, Braslawsky G, White C, et al. Antibody therapy of non-Hodgkin's B-cell lymphoma. Cancer Immunol Immunother 2003;52:257–80.
5. Banchereau J, Bazan F, Blanchard D, et al. The CD40 antigen and its ligand. Annu Rev Immunol 1994;12:881–922.
6. van Kooten C, Banchereau J. Functions of CD40 on B cells, dendritic cells and other cells. Curr Opin Immunol 1997;9:330–7.
7. Young LS, Eliopoulos AG, Gallagher NJ, et al. CD40 and epithelial cells: across the great divide. Immunol Today 1998;19:502–6.
8. van Kooten C, Banchereau J. CD40-CD40 ligand. J Leukoc Biol 2000;67:2–17.
9. Uckun FM, Gajl-Peczalska K, Myers DE, et al. Temporal association of CD40 antigen expression with discrete stages of human B-cell ontogeny and the efficacy of anti-CD40 immunotoxins against clonogenic B-lineage acute lymphoblastic leukemia as well as B-lineage non-Hodgkin's lymphoma cells. Blood 1990;76:2449–56.
10. O'Grady JT, Stewart S, Lowrey J, et al. CD40 expression in Hodgkin's disease. Am J Pathol 1994;144:21–6.
11. Westendorf JJ, Ahmann GJ, Armitage RJ, et al. CD40 expression in malignant plasma cells. Role in stimulation of autocrine IL-6 secretion by a human myeloma cell line. J Immunol 1994;152:117–28.
12. Ziebold JL, Hixon J, Boyd A, et al. Differential effects of CD40 stimulation on normal and neoplastic cell growth. Arch Immunol Ther Exp (Warsz) 2000;48:225–33.

13. Ottaiano A, Pisano C, De Chiara A, et al. CD40 activation as potential tool in malignant neoplasms. Tumori 2002;88:361–6.
14. Grewal IS, Flavell RA. CD40 and CD154 in cell-mediated immunity. Annu Rev Immunol 1998;16:111–35.
15. Clark EA, Ledbetter JA. How B and T cells talk to each other. Nature 1994;367:425–8.
16. Aruffo A, Farrington M, Hollenbaugh D, et al. The CD40 ligand, gp39, is defective in activated T cells from patients with X-linked hyper-IgM syndrome. Cell 1993;72:291–300.
17. Hayward AR, Levy J, Facchetti F, et al. Cholangiopathy and tumors of the pancreas, liver, and biliary tree in boys with X-linked immunodeficiency with hyper-IgM. J Immunol 1997;158:977–83.
18. Kinlen LJ, Webster AD, Bird AG, et al. Prospective study of cancer in patients with hypogammaglobulinaemia. Lancet 1985;1:263–6.
19. Laman JD, Claassen E, Noelle RJ. Immunodeficiency due to a faulty interaction between T cells and B cells. Curr Opin Immunol 1994;6:636–41.
20. Costello RT, Gastaut JA, Olive D. What is the real role of CD40 in cancer immunotherapy? Immunol Today 1999;20:488–93.
21. Ranheim EA, Kipps TJ. Activated T cells induce expression of B7/BB1 on normal or leukemic B cells through a CD40-dependent signal. J Exp Med 1993;177: 925–35.
22. Funakoshi S, Longo DL, Beckwith M, et al. Inhibition of human B-cell lymphoma growth by CD40 stimulation. Blood 1994;83:2787–94.
23. Szocinski JL, Khaled AR, Hixon J, et al. Activation-induced cell death of aggressive histology lymphomas by CD40 stimulation: induction of bax. Blood 2002;100: 217–23.
24. Wang D, Freeman GJ, Levine H, et al. Role of the CD40 and CD95 (APO-1/Fas) antigens in the apoptosis of human B-cell malignancies. Br J Haematol 1997;97: 409–17.
25. Francisco JA, Donaldson KL, Chace D, et al. Agonistic properties and *in vivo* antitumor activity of the anti-CD40 antibody SGN-14. Cancer Res 2000;60:3225–31.
26. Paulie S, Koho H, Ben Aissa H, et al. Monoclonal antibodies to antigens associated with transitional cell carcinoma of the human urinary bladder. II. Identification of the cellular target structures by immunoprecipitation and SDS-PAGE analysis. Cancer Immunol Immunother 1984;17:173–9.
27. Paulie S, Ehlin-Henriksson B, Mellstedt H, et al. A p50 surface antigen restricted to human urinary bladder carcinomas and B lymphocytes. Cancer Immunol Immunother 1985;20:23–8.
28. Malmborg Hager AC, Ellmark P, Borrebaeck CA, et al. Affinity and epitope profiling of mouse anti-CD40 monoclonal antibodies. Scand J Immunol 2003;57: 517–24.
29. Pound JD, Challa A, Holder MJ, et al. Minimal cross-linking and epitope requirements for CD40-dependent suppression of apoptosis contrast with those for promotion of the cell cycle and homotypic adhesions in human B cells. Int Immunol 1999;11:11–20.
30. Hayashi T, Treon SP, Hideshima T, et al. Recombinant humanized anti-CD40 monoclonal antibody triggers autologous antibody-dependent cell-mediated cytotoxicity against multiple myeloma cells. Br J Haematol 2003;121:592–6.
31. Roder JC. The beige mutation in the mouse. I. A stem cell predetermined impairment in natural killer cell function. J Immunol 1979;123:2168–73.
32. Roder JC, Lohmann-Matthes ML, Domzig W, et al. The beige mutation in the mouse. II. Selectivity of the natural killer (NK) cell defect. J Immunol 1979;123:2174–81.
33. Tai YT, Catley LP, Mitsiades CS, et al. Mechanisms by which SGN-40, a humanized anti-CD40 antibody, induces cytotoxicity in human multiple myeloma cells: clinical implications. Cancer Res 2004;64:2846–52.
34. Carnahan J, Wang P, Kendall R, et al. Epratuzumab, a humanized monoclonal antibody targeting CD22: characterization of in vitro properties. Clin Cancer Res 2003;9:3982–90S.
35. Inui S, Kaisho T, Kikutani H, et al. Identification of the intracytoplasmic region essential for signal transduction through a B cell activation molecule, CD40. Eur J Immunol 1990;20:1747–53.
36. Heath AW, Chang R, Harada N, et al. Antibodies to murine CD40 stimulate normal B lymphocytes but inhibit proliferation of B lymphoma cells. Cell Immunol 1993;152:468–80.
37. Hollmann AC, Gong Q, Owens T. CD40-mediated apoptosis in murine B-lymphoma lines containing mutated p53. Exp Cell Res 2002;280:201–11.
38. Hess S, Engelmann H. A novel function of CD40: induction of cell death in transformed cells. J Exp Med 1996;183:159–67.
39. Eliopoulos AG, Davies C, Knox PG, et al. CD40 induces apoptosis in carcinoma cells through activation of cytotoxic ligands of the tumor necrosis factor superfamily. Mol Cell Biol 2000;20:5503–15.
40. Gallagher NJ, Eliopoulos AG, Agathangelo A, et al. CD40 activation in epithelial ovarian carcinoma cells modulates growth, apoptosis, and cytokine secretion. Mol Pathol 2002;55:110–20.
41. Teoh G, Tai YT, Urashima M, et al. CD40 activation mediates p53-dependent cell cycle regulation in human multiple myeloma cell lines. Blood 2000;95: 1039–46.
42. Aggarwal BB. Signalling pathways of the TNF superfamily: a double-edged sword. Nat Rev Immunol 2003;3:745–56.
43. Harnett MM. CD40: a growing cytoplasmic tale. Sci STKE 2004;2004:pe25.
44. Mitsiades N, Mitsiades CS, Poulaki V, et al. Apoptotic signaling induced by immunomodulatory thalidomide analogs in human multiple myeloma cells: therapeutic implications. Blood 2002;99:4525–30.
45. Voorhees PM, Dees EC, O'Neil B, et al. The proteasome as a target for cancer therapy. Clin Cancer Res 2003;9:6316–25.
46. Mathas S, Lietz A, Janz M, et al. Inhibition of NF-κB essentially contributes to arsenic-induced apoptosis. Blood 2003;102:1028–34.
47. Funakoshi S, Longo DL, Murphy WJ. Differential *in vitro* and *in vivo* antitumor effects mediated by anti-CD40 and anti-CD20 monoclonal antibodies against human B-cell lymphomas. J Immunother Emphasis Tumor Immunol 1996;19:93.
48. Funakoshi S, Beckwith M, Fanslow W, et al. Epstein-Barr virus-induced human B-cell lymphoma arising in HuPBL-SCID chimeric mice: characterization and the role of CD40 stimulation in their treatment and prevention. Pathobiology 1995;63:133–42.
49. Murphy WJ, Funakoshi S, Beckwith M, et al. Antibodies to CD40 prevent Epstein-Barr virus-mediated human B-cell lymphomagenesis in severe combined immune deficient mice given human peripheral blood lymphocytes. Blood 1995;86:1946–53.
50. Clynes RA, Towers TL, Presta LG, et al. Inhibitory Fc receptors modulate *in vivo* cytoxicity against tumor targets. Nat Med 2000;6:443–6.
51. Cartron G, Dacheux L, Salles G, et al. Therapeutic activity of humanized anti-CD20 monoclonal antibody and polymorphism in IgG Fc receptor *FcγRIIIa* gene. Blood 2002;99:754–8.
52. Weng WK, Levy R. Two immunoglobulin G fragment C receptor polymorphisms independently predict response to rituximab in patients with follicular lymphoma. J Clin Oncol 2003;21:3940–7.

Antilymphoma Activity of an Anti-CD40 Antibody

In the article on antilymphoma activity of an anti-CD40 antibody in the September 15, 2005 issue of *Cancer Research* (1), there is an error in Fig. 4. The key to Fig. 4*A* should read that the blue lines represent the binding of anti-CD40 antibody and that the red lines represent the binding of anti-CD20 antibody.

1. Law C-L, Gordon KA, Collier J, Klussman K, McEarchern JA, Cerveny CG, Mixan BJ, Lee WP, Lin Z, Valdez P, Wahl AF, Grewal IS. Preclinical antilymphoma activity of a humanized anti-CD40 monoclonal antibody, SGN-40. Cancer Res 2005;65:8331–8.

doi:10.1158/0008-5472.CAN-66-4-COR

Preclinical Antilymphoma Activity of a Humanized Anti-CD40 Monoclonal Antibody, SGN-40

Che-Leung Law, Kristine A. Gordon, John Collier, et al.

Cancer Res 2005;65:8331-8338.